37. S. Oldham, E. Hafen, unpublished results.
38. A. Arcaro, M. P. Wymann, *Biochem. J.* **296**, 297 (1993).
39. M. Andjelkovic *et al.*, *J. Biol. Chem.* **272**, 31515 (1997).
40. M. Andjelkovic *et al.*, *J. Biol. Chem.* **270**, 4066 (1995).
41. Single-letter abbreviations for the amino acid residues are as follows: A, Ala; E, Glu; F, phe; G, Gly; I, Ile; P, Pro; R, Arg; S, Ser; and T, Thr.
42. dAkt was immunoprecipitated from wild-type and *dAkt*^{3} larvae with a rabbit polyclonal antibody raised against recombinant dAkt-66 (*40*). In vitro kinase assays were performed, as described, using the peptide GRPRTSSAEG (*41*) as a substrate (*39*).
43. HEK 293 cells were transfected by a modified calcium phosphate method, as described (*39*). The transfection mixture was removed after a 16-hour incubation, and cells were serum-starved for 24 hours before stimulation with 0.5 to 1 μM insulin (Boehringer Mannheim).
44. The HA epitope–tagged dAkt proteins were immunoprecipitated from 100 μg of cell-free extracts using the monoclonal antibody 12CA5 coupled to protein A–Sepharose. In vitro kinase assays were performed, as described (*39*).
45. The size difference of the eyes in Fig. 4, B and D, is entirely due to varying numbers of ommatidia. The size of the ommatidia, however, is comparable (insets) and massively larger than in *chico* mutants (inset in 4C). The failure of myr-dAkt to compensate for the reduced number of ommatidia in *chico* mutants is consistent with the late onset of expression driven by *GMR-Gal4*.
46. We thank Ch. Zuker and E. Koundakjian for the *dAkt*^{3} allele; T. Radimerski for the S2 labeling medium; T. Gutjahr, Ch. Hugentobler, R. Bopp, P. Zipperlen, P. Cron, P. Müller, and H. Angliker for technical support; K. Basler and P. Gallant for critical reading of the manuscript and valuable suggestions; and D. Pan and S. Leevers for providing fly stocks. Supported by grants from the Schweizerische Krebsliga (B.A.H. and M.P.W.) and the Swiss National Science Foundation (E.H.).

15 November 2001; accepted 12 February 2002

Reverse Transcriptase–Mediated Tropism Switching in *Bordetella* Bacteriophage

Minghsun Liu,[1] Rajendar Deora,[1]* Sergei R. Doulatov,[1]* Mari Gingery,[1] Frederick A. Eiserling,[1] Andrew Preston,[2] Duncan J. Maskell,[2] Robert W. Simons,[1] Peggy A. Cotter,[3] Julian Parkhill,[4] Jeff F. Miller[1]†

Host-pathogen interactions are often driven by mechanisms that promote genetic variability. We have identified a group of temperate bacteriophages that generate diversity in a gene, designated *mtd* (major tropism determinant), which specifies tropism for receptor molecules on host *Bordetella* species. Tropism switching is the result of a template-dependent, reverse transcriptase–mediated process that introduces nucleotide substitutions at defined locations within *mtd*. This cassette-based mechanism is capable of providing a vast repertoire of potential ligand-receptor interactions.

The infectious cycles of *Bordetella* subspecies, which cause respiratory infections in humans and other mammals, is controlled by the BvgAS signal transduction system (*1*). Using a multistep phosphorelay, the BvgS transmembrane sensor-kinase and the BvgA transcriptional regulator couple environmental signals to expression of cell surface and secreted molecules (*1*, *2*). The Bvg$^+$ phase, which is necessary and sufficient for respiratory tract colonization, is characterized by a high level of BvgAS activity and expression of virulence and colonization factors that include adhesins, toxins, and a type III secretion system (*2*). In the Bvg$^-$ phase, BvgAS is inactive, virulence and colonization factors are not expressed, and numerous genes are induced, including motility loci in *Bordetella bronchiseptica* and virulence repressed genes in *Bordetella pertussis* (*2*, *3*). The Bvg$^-$ phase appears to be adapted to ex vivo growth and survival in *B. bronchiseptica* (*4*). Recent evidence suggests that BvgAS is capable of controlling a spectrum of distinct phenotypic phases in response to subtle changes in signal intensity (*5*, *6*).

In a search for generalized transducing vectors, we identified several temperate bacteriophages present in clinical isolates of *B. bronchiseptica* that displayed a marked tropism for Bvg$^+$ as opposed to Bvg$^-$ phase bacteria. The efficiency of plaque formation of a representative phage, designated BPP-1 (Bvg plus tropic phage–1), was 10^6-fold higher on Bvg$^+$ phase RB50 (wild-type *B. bronchiseptica*) than on an isogenic Bvg$^-$ phase-locked strain (Δ*bvgS*) (Fig. 1A). An adsorption assay (Fig. 1B) indicated that the BPP-1 receptor is specifically expressed in the Bvg$^+$ phase. Mutagenesis of loci encoding Bvg$^+$ phase surface factors showed that deletion of *prn*, which encodes the adhesin pertactin (*7*), eliminated BPP-1 adsorption and decreased phage plaquing to a level similar to that observed on Bvg$^-$ phase cells (Fig. 1, A and B). Ectopic expression of *prn*

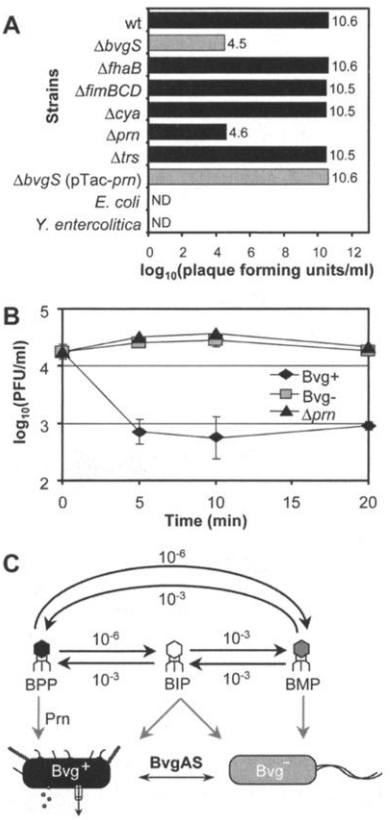

Fig. 1. (**A**) Efficiency of plaquing by a high-titer BPP-1 lysate [4×10^{10} plaque forming units/ml (pfu/ml)] on isogenic *B. bronchiseptica* mutants. The Δ*bvgS*, Δ*fhaB*, Δ*fimBCD*, Δ*cyaA*, Δ*prn*, and Δ*trs* mutations are in-frame deletion mutations that eliminate BvgS activity or expression of FHA (filamentous hemagglutinin), fimbriae, adenylate cyclase toxin, pertactin, or the type III secretion apparatus. Black bars indicate Bvg$^+$ phase strains; gray bars indicate strains genetically locked in the Bvg$^-$ phase. pTac-prn is a complementing plasmid that expresses pertactin under control of the Tac promoter. *E. coli* strain DH5α and *Yersinia enterocolitica* strain JB580v did not support phage growth. ND, no plaque detected. (**B**) BPP-1 adsorption assay (*8*) with the use of wild-type *B. bronchiseptica* strain RB50 (*4*), isogenic Bvg$^-$ (Δ*bvgS*), and Δ*prn* derivatives, all grown under Bvg$^+$ phase conditions. (**C**) Summary of tropism switching frequencies by *Bordetella* phages. A spontaneous mutant resistant to BIP-1 but still sensitive to BPP-1 and BMP-1 were used to obtain switching frequencies from BIP-1 to BPP or BMP tropic variants.

[1]Department of Microbiology, Immunology and Molecular Genetics, University of California, Los Angeles, Los Angeles, CA 90095, USA. [2]Centre for Veterinary Science, Department of Clinical Veterinary Medicine, University of Cambridge, Cambridge CB3 OES, UK. [3]Department of Molecular, Cellular and Developmental Biology, University of California, Santa Barbara, Santa Barbara, CA 93106, USA. [4]The Sanger Centre, The Wellcome Trust Genome Campus, Hixton, Cambridge, UK.

*These authors contributed equally to this work.
†To whom correspondence should be addressed. E-mail: jfmiller@ucla.edu.

in a Δ*bvgS* strain was sufficient to confer full infectivity by BPP-1 (Fig. 1A), indicating that pertactin is the primary determinant of BPP-1 tropism.

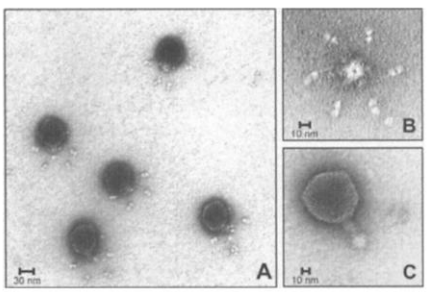

Fig. 2. Transmission electron microscopy. (**A**) BPP-1 particles. BPP-1, BMP-1, and BIP-1 are identical in morphology by electron microscopy. (**B**) BPP-1 base plate and tail fibers. (**C**) BPP-1ΔVR1. Bar in (A), 30 nm; bars in (B) and (C), 10 nm.

Although the BPP-1 efficiency of plaquing decreased by a factor of 10^6 on Bvg^- phase cells (Fig. 1A), plaques that did form had a normal morphology. Because plaque formation requires multiple rounds of phage infection and multiplication, this observation suggested that a tropism switch had occurred (*8*). Two types of tropic variants were identified [Web fig. 1 (*8*)]. The first, designated BMP (Bvg minus tropic phage) switched tropism to favor Bvg^- phase *Bordetella*. The second, designated BIP (Bvg indiscriminant phage), formed plaques with nearly equal efficiency on Bvg^+ or Bvg^- phase strains. The three variants are capable of converting between different tropisms at characteristic frequencies (Fig. 1C), and in all cases phage tropism correlated with specific adsorption to bacterial cell surfaces (*9*). Thus, these bacteriophages have evolved a mechanism for adapting to cell surface alterations that occur during the infectious cycles of their hosts.

Electron microscopy did not reveal gross morphologic differences between phage variants. Viral particles consisted of an icosahedral head, a short neck, and six tail fibers with unusual globular structures at each distal end (Fig. 2, A and B). Comparison of the 42.5 kilobase (kb) double-stranded DNA (dsDNA) genomes of BPP-1, BIP-1, and BMP-1 revealed a region of variability, VR1, which differed between tropic variants (Fig. 3A). VR1 consists of a 134–base pair (bp)–repeated sequence located at the extreme 3′ end of the *mtd* (major tropism determinant) locus, which encodes a 40-kD polypeptide (*10*). Over 90% of the changes detected in a sample of 21 tropic variants occurred at 22 discrete positions within VR1 [Fig. 3D; Web figs. 2 and 3 (*8*)]. Variability hotspots were almost always located in the first two bases of predicted codons, thereby maximizing the

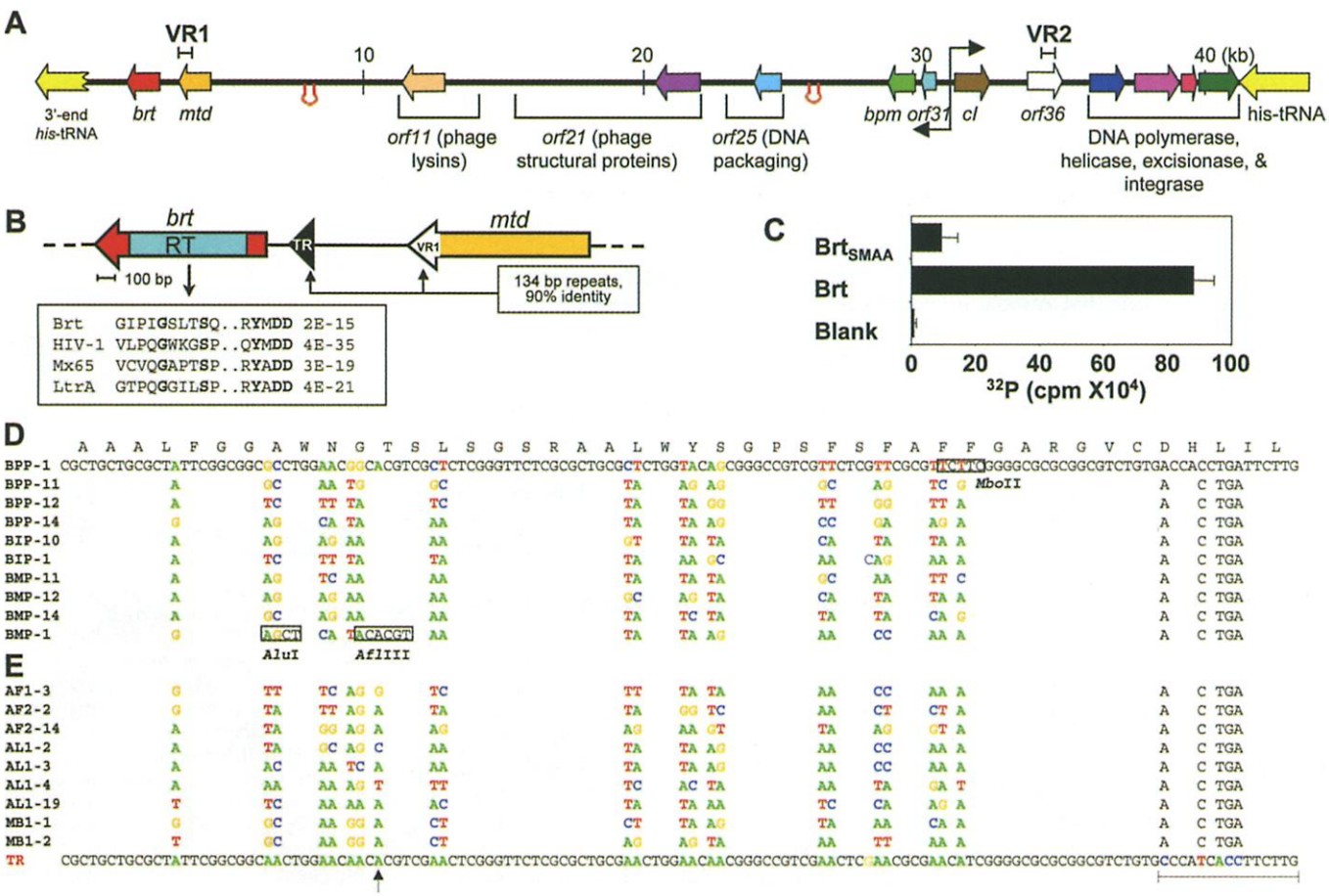

Fig. 3. (**A**) Schematic of the integrated *Bordetella* phage genome. The unannotated sequence is available from the Sanger Centre Web site at www.sanger. ac.uk/Projects/B_pertussis/. Further information is available in the supplementary material (*8*). (**B**) Organization of the *mtd*, VR1, TR, and *brt* loci. Alignments of highly conserved residues, including the YXDD motif, in the reverse transcriptase domains of Brt, HIV-1 RT, Mx65, and LtrA of the *Lactococcus lactis* Ll.LtrB group II intron (GenBank accession numbers are 1065287, 134074, and AAB06503, respectively) are shown. The Pfam RT domain (GenBank accession number PF00078) E value is shown next to each sequence. (**C**) RT activity of purified Brt protein and the YMDD to SMAA mutant derivative (Brt$_{SMAA}$) with the use of poly(rA) as a template primed with an oligo(dT)$_{18}$ primer. His$_6$-tagged derivatives of the wild-type Brt protein and the Brt$_{SMAA}$ mutant were purified and RT activity was measured as described (*12*). Incorporation of [α-^{32}P]dTTP in 10 μl reactions (at 37°C for 15 min with 20 ng of recombinant protein) is shown. The blank contained boiled protein and RNase H$^-$ MMLV RT was used as a positive control. (**D**) VR1 sequences of allthree classes of phage tropic variants selected in vivo (*8*). (**E**) VR1 sequences selected with the use of the restriction enzyme-based variability assay (*13*). Restriction sites used for selecting the variant sequences are shown in boxes. All sequences are aligned with VR1 of BPP-1 (top) and TR (bottom). Nucleotides in highly variable positions are shown in bold and are color-coded. An expanded data set and phage pedigree are available in the supplementary information [Web figs. 2 and 3 (*8*)].

potential to generate amino acid substitutions. The number of nucleotide differences observed between phages with different tropisms ranged from 4 to 19, resulting in amino acid differences ranging from 3 to 17. We have never observed identical VR1 sequences (nucleotide or predicted amino acid) among independently derived phages. Located downstream from *mtd* is a second copy of the 134-bp repeat, called the template repeat (TR), which is approximately 90% identical to VR1 (Fig. 3B). In contrast to VR1, TR never varied when sequences of phage with similar or different tropisms were compared. Adjacent to TR is a locus, designated *brt* (*Bordetella* reverse transcriptase), which encodes an enzymatically active reverse transcriptase (RT) with sequence similarity to the RT domains of group II intron maturases, bacterial retrons, and retroviral reverse transcriptases (Fig. 3, B and C). The presence of a reverse transcriptase in a dsDNA phage and its proximity to VR1 raised the possibility that reverse transcription plays a role in generating host range alterations.

We constructed a series of in-frame deletion and substitution mutations to determine the roles of VR1, the TR element, and the *brt* locus in phage infectivity and tropism switching (Table 1) (*11*). In-frame deletion of VR1 eliminated phage infectivity and resulted in phage particles that lacked tail fibers and had extended neck structures (Fig. 2C), consistent with a role of the *mtd* product in tail fiber assembly. In contrast, deletion mutations in the *brt* loci of Bvg^+ and Bvg^- tropic variants resulted in fully infective phages that had completely lost the ability to switch tropism. Altering the conserved reverse transcriptase motif (YMDD to SMAA) eliminated Brt activity in vitro (Fig. 3C) (*12*) and tropism switching in vivo (Table 1). Thus, tropism switching is a reverse transcriptase–mediated event. Substituting VR1 sequences between Δ*brt* phages with different tropisms demonstrated that VR1 is sufficient to determine host specificity (Table 1) (*8*).

As shown in Table 1, phages containing deletion mutations that precisely eliminate TR had phenotypes identical to mutants defective in the phage-encoded RT, namely, a complete absence of tropism switching. We next tested the possibility that the TR serves as a template for generating diversity in VR1. A single nucleotide substitution was introduced into the TR of BPP-1 at a site corresponding to an invariant position in VR1 [Web fig. 4A (*8*)]. The substitution did not alter the predicted amino acid encoded by the equivalent codon in VR1. In a sample of 56 derivatives that had switched tropism, 93% contained the silent substitution at the corresponding site in VR1 as well as sequence alterations at variable sites characteristic of tropism switching. Progeny that had not switched tropism did not contain the substitution or any other changes in VR1. Similar results were obtained with the use of a different silent substitution in the BMP-1 background [Web fig. 4B (*8*)]. These results demonstrate that information is transferred from TR to VR1 during a tropism switch and that TR functions as an essential template for the variability-generating mechanism.

The variability assessments in Fig. 3D are biased by a requirement for infectious phages. Although they suggest a process that is relatively or exclusively site specific, the data are also consistent with the possibility that the diversity-generating mechanism introduces random mutations across VR1 and that the observed hotspots are a result of selection. To differentiate between these possibilities, we devised an assay for variability that is independent of phage infectivity, but relies on the ability of variations in VR1 to eliminate restriction enzyme recognition sites and protect PCR products from cleavage (*13*). As shown in Fig. 3E, sites of variability identified with this restriction enzyme-based selection were nearly identical to those observed by selecting for infectious phage variants (Fig. 3D). Thus, the diversity-generating mechanism targets a subset of positions within VR1. Furthermore, the majority of nucleotide substitutions in VR1 occur at positions that correspond to adenine residues in the TR. With the exception of a 15-bp sequence at the 3′ end of TR, every adenine residue within TR corresponds to a variable position in VR1. We conclude that hotspots for variability observed in VR1 reflect a fundamental nucleotide preference inherent in the diversity-generating process.

Our genetic analysis suggests a likely sequence of events for RT-mediated variability in *Bordetella* phages [Web fig. 5 (*8*)]. The apparent requirement for RT activity implicates an RNA species as an essential intermediate. Deletion and substitution mutagensis of TR suggests that a TR-derived transcript serves as the template for reverse transcription and mutagenesis. Although the mechanisms of cDNA priming and mutagenesis are unknown, the correspondence between variable sites in VR1 and A:T base pairs in the TR is consistent with sequence-dependent misincorporation, as has been demonstrated with HIV-RT (*14*). Specific nucleotide modifications, such as those catalyzed by adenosine deaminases (*15*), would provide an alternative means for mutagenesis. A mechanism that allows the proposed TR-derived cDNA product to substitute for existing VR1 sequences is also required. By analogy with the site-specific retrohoming ability of group II introns (*16*), endonucleolytic cleavage of the recipient DNA by an accessory domain of the phage RT or by an unidentified gene product may also be necessary for tropism switching.

Although VR1 determines phage tropism and the *mtd* product is predicted to be involved in receptor recognition, alignment and analysis of sequences from phage variants did not reveal an association (charge, hydrophobicity, or amino acid similarity) between amino acid patterns in VR1 and particular host specificities. The interactions between *Bordetella* phages and their respective receptors appear to be more complex than can be captured by simply classifying phages into three different tropisms. Indeed, Bvg^+ phase-specific phages capable of infecting Δ*prn* mutants have been isolated (*17*). These and other results indicate that a variety of bacterial receptors can be used by different tropic variants.

Table 1. Summary of *Bordetella* phage mutants. Phage titers were determined on Bvg^+ and Bvg^- phase bacteria after induction with mitomycin C ($\sim 10^{11}$ pfu/ml for functional phages), and for each strain the higher of two titers is set arbitrarily to 1.0. ND designates that no phages were detected. Relative efficiencies of plaquing of $<10^{-11}$ indicate that no tropic variants were found. Additional experimental details are available in supplementary information (*8*).

Phage	Relative plaquing efficiency	
	Bvg^+	Bvg^-
BPP-1	1.0	7.9×10^{-7}
BMP-1	7.4×10^{-4}	1.0
BPP-1ΔVR1	ND	ND
BMP-1ΔVR1	ND	ND
BIP-1ΔVR1	ND	ND
BPP-1Δ*brt*	1.0	$<10^{-11}$
BMP-1Δ*brt*	$<10^{-11}$	1.0
BPP-1-brt_{SMAA}	1.0	$<10^{-11}$
BMP-1-brt_{SMAA}	$<10^{-11}$	1.0
BPP-1Δ*brt*($VR1_{BMP-1}$)	$<10^{-11}$	1.0
BPP-1Δ*brt*($VR1_{BIP-1}$)	1.0	1.0
BMP-1Δ*brt*($VR1_{BPP-1}$)	1.0	$<10^{-11}$
BPP-1ΔTR	1.0	$<10^{-11}$
BMP-1ΔTR	$<10^{-11}$	1.0

The variability-generating system is theoretically capable of generating over 7.0×10^{13} different nucleotide sequences and 9.2×10^{12} amino acid sequences in VR1 and the encoded product, respectively (*18*). The close proximity of required genetic elements suggests that it operates as a variability-generating cassette with three major components: a reverse transcriptase, a template repeat, and a second repeated sequence capable of variation. A more detailed understanding of the variability mechanism should allow us to engineer constructs designed to promote in vivo targeted mutagenesis of specific DNA sequences. Such capability could be useful in applications where massive parallel screening of diverse protein sequences is desirable.

Reverse transcriptases are ubiquitous in nature. They are frequently found in both prokaryotic and eukaryotic genomes and are often associated with mobile genetic elements (*19*). Indeed, over 40% of the human genome appears to have resulted from the process of reverse transcription (*20*). Variations of the RT-dependent diversity-generating mechanism described here could confer powerful selective advantages in a variety of biological contexts. It will be of interest to determine if this adaptive mechanism has found utility in nature in addition to its role in facilitating tropism switching by *Bordetella* bacteriophages.

References and Notes

1. M. A. Uhl, J. F. Miller, *EMBO J.* **15**, 1028 (1996).
2. P. A. Cotter, J. F. Miller, in Principles of Bacterial Pathogenesis, E. A. Groisman, Ed. (Academic Press, San Diego, 2001), pp. 620–674.
3. B. J. Akerley, P. A. Cotter, J. F. Miller, *Cell* **80**, 611 (1995).
4. P. A. Cotter, J. F. Miller, *Mol. Microbiol.* **24**, 671 (1997).
5. K. E. Stockbauer, B. Fuchslocher, J. F. Miller, P. A. Cotter, *Mol. Microbiol.* **39**, 65 (2001).
6. R. Deora, H. J. Bootsma, J. F. Miller, P. A. Cotter, *Mol. Microbiol.* **40**, 669 (2001).
7. E. Leininger *et al.*, *Proc. Natl. Acad. Sci. U.S.A.* **88**, 345 (1991).
8. Supplemental information is available on *Science* Online at www.sciencemag.org/cgi/content/full/295/5562/2091/DC1.
9. M. Liu, S. Doulatov, J. F. Miller, data not shown.
10. To identify the *mtd*-encoded polypeptide, rabbit antibody was raised against a recombinant glutathione S-transferase–Mtd (GST-Mtd) fusion protein. Western blotting of concentrated phage lysates resulted in recognition of a 40-kD protein corresponding to the predicted size of Mtd. No significant similarity to *mtd* was found in GenBank database. Annotation of the phage genome did not reveal any other predicted open reading frames (ORFs) with similarity to known bacteriophage tail fiber proteins.
11. In-frame deletions were carried out using allelic exchange essentially as described by R. A. Edwards, L. H. Keller, and D. M. Schifferli [*Gene* **207**, 149 (1998)].
12. His_6-tagged derivatives of the wild-type Brt protein and the YMDD to SMAA mutant (Brt_{SMAA}) were constructed, overexpressed in *E. coli*, and purified from insoluble inclusion bodies. [Single-letter abbreviations for the amino acid residues are as follows: A, Ala; C, Cys; D, Asp; E, Glu; F, Phe; G, Gly; H, His; I, Ile; K, Lys; L, Leu; M, Met; N, Asn; P, Pro; Q, Gln; R, Arg; S, Ser; T, Thr; V, Val; W, Trp; and Y, Tyr.] Proteins were solubilized with the use of 6 M guanidine hydrochloride and renatured in the presence of 1 M nondetergent sulfobetaines (Novagen, Madison, WI) and dialyzed overnight in 40 mM Tris pH 8.0, 10 mM $MgCl_2$, 2 mM dithiothreitol (DTT), and 50% glycerol. RT assays were performed essentially as described by M. Matsuura *et al.* [*Genes Dev.* **11**, 2910 (1997)] with the use of poly(rA) as the template primed with oligo$(dT)_{18}$ primers.
13. BPP-1 or BMP-1 lysogens were induced with mitomycin C to eliminate selection for infectious phages. The lysates were used to generate polymerase chain reaction (PCR) products containing VR1, which were purified and digested with Afl III or Alu I for BMP-1 or with Mbo II for BPP-1. The amplification-restriction cycle was repeated until no further cutting was observed, and the products were cloned into pBluescript KS+ for sequencing. See supplementary information (*8*) for the primers used.
14. H. Doi, *Proc. Natl. Acad. Sci. U.S.A.* **88**, 9282 (1991).
15. E. A. P. Gerber, W. Keller, *Trends Biochem. Sci.* **26**, 376 (2001).
16. F. Martinez-Abarca, N. Toro, *Mol. Microbiol.* **38**, 917 (2000).
17. S. Doulatov, J. F. Miller, unpublished results.
18. At the nucleotide level, variations were consistently seen at 23 positions in VR1 and, in most cases, all four nucleotides were observed [Web fig. 2 (*8*)]. Therefore, the maximum theoretical diversity is $4^{23} = 7 \times 10^{13}$. Of the 23 variable bases, 20 are distributed in 10 separate dinucleotides capable of encoding one of 15 possible amino acids, and 2 are in the first base of a codon. The theoretical amino acid diversity is then $15^{10} \times 4^2 = 9.2 \times 10^{12}$.
19. M. F. Singer, *J. Biol. Chem.* **270**, 24623 (1995).
20. E. S. Lander *et al.*, *Nature* **409**, 860 (2001).

21. We would like to thank the members of the Miller lab for helpful comments throughout the course of this work. M.L. was supported by a research fellowship from the American Lung Association and a training grant GM-08042 to the UCLA-CalTech Medical Scientist Training Program from the NIH. This work was supported by NIH grants AI38417 (J.F.M.), AI43986 (P.A.C.), and T32A107323 (R.D.) and by USDA grant 1999-02298 (J.F.M and P.A.C). The sequencing of BPP-1, BMP-1, and BIP-1 genomes were supported by the Wellcome Trust.

26 October 2001; accepted 24 January 2002

Influence of SHIP on the NK Repertoire and Allogeneic Bone Marrow Transplantation

Jia-Wang Wang,[1]* Julie M. Howson,[1]* Tomar Ghansah,[1]* Caroline Desponts,[1] John M. Ninos,[1] Sarah L. May,[1] Kim H. T. Nguyen,[1] Noriko Toyama-Sorimachi,[2] William G. Kerr[1]†

Natural killer cell (NK) receptors for major histocompatibility complex (MHC) class I influence engraftment and graft-versus-tumor effects after allogeneic bone marrow transplantation. We find that SH2-containing inositol phosphatase (SHIP) influences the repertoire of NK receptors. In adult $SHIP^{-/-}$ mice, the NK compartment is dominated by cells that express two inhibitory receptors capable of binding either self or allogeneic MHC ligands. This promiscuous repertoire has significant functional consequences, because $SHIP^{-/-}$ mice fail to reject fully mismatched allogeneic marrow grafts and show enhanced survival after such transplants. Thus, SHIP plays an important role in two processes that limit the success of allogeneic marrow transplantation: graft rejection and graft-versus-host disease.

Certain intracellular phosphatases contain SH2 domains that enable their recruitment to phosphorylated tyrosine residues in the cytoplasmic tails of inhibitory receptors (*1*). Following recruitment to the plasma membrane, these enzymes remove phosphate groups on other proteins or inositol phospholipids and thus counteract signaling cascades necessary for cell survival, proliferation or differentiation. SHIP is one of these signaling phosphatases (*2–4*). SHIP has been shown to limit the number of myeloid cells produced in vivo demonstrating it as a crucial mediator of survival signals in a hematopoietic lineage (*5, 6*).

In order to examine the role SHIP plays in NK development and function, we generated mice with a targeted mutation in the SHIP gene resulting in SHIP-deficient mice (*7*). Analysis of the peripheral NK compartment at different stages of ontogeny (*7*) indicated NK cells develop normally in juvenile $SHIP^{-/-}$ mice (Fig. 1A). However, in adult mice an abnormal population of NK cells appears that expresses approximately 10-fold higher surface levels of the NK receptor, NK1.1 ($NK1.1^{hi}$) (Fig. 1A). The $NK1.1^{hi}$ population lacks CD3 and thus is not an NK-T cell population. The appearance of the

[1]Immunology Program, H. Lee Moffitt Comprehensive Cancer Center and Research Institute, and Departments of Interdisciplinary Oncology and Biochemistry, University of South Florida, Tampa, FL 33612, USA. [2]Department of Immune Regulation, Tokyo Medical and Dental University, Tokyo 113-8150, Japan.

*These authors contributed equally to this work.
†To whom correspondence should be addressed. E-mail: kerrw@moffitt.usf.edu